

An Electrochemical Study of Surface Oxidation and Collectorless Flotation of Pyrite

Dongping Tao^{1,*}, Yue Wang¹ and Lin Li²

¹ School of Mining Engineering, University of Science and Technology Liaoning, Anshan, Liaoning 114051, China.

² College of Chemical and Environmental Engineering, Shandong University of Science and Technology, Qingdao, Shandong 266590, China

*E-mail: dptao@qq.com

Received: 27 October 2017 / Accepted: 6 April 2018 / Published: 10 May 2018

Pyrite is a common sulfide mineral and its surface oxidation and natural hydrophobicity play an important role in determining flotation performance for many minerals, particularly for sulfides and coal. In this study freshly fractured electrodes have been used to investigate the surface oxidation of fresh pyrite surface and collectorless microflotation tests were performed to study its natural hydrophobicity. Chronoamperometry performed on in-situ fractured electrodes demonstrated that pyrite oxidation takes place at potentials of -0.28 V (SHE) at pH 9.2 and 0 V at pH 4.6, considerably lower than previously assumed. Incipient oxidation at slightly more positive potentials produce a hydrophobic sulfur-rich species, most likely a polysulfide or metal-deficient sulfide, which imparts natural surface hydrophobicity to pyrite. Collectorless microflotation test results have indicated that pyrite acquires considerable floatability upon superficial oxidation. The collectorless flotation recovery of pyrite is determined by the relative amounts of polysulfide, soluble species, and insoluble species produced during oxidation, which depends on solution pH and potential.

Keywords: chronoamperometry, collectorless flotation, freshly fractured electrodes, hydrophobicity, oxidation, pyrite, voltammetry

1. INTRODUCTION

Pyrite is one of the most common sulfide minerals encountered in the mining and mineral industry. It often co-exists with other sulfide minerals such as chalcopyrite, sphalerite and galena [1-2] and non-sulfide minerals including coal in which it is considered a gangue mineral and thus rejected as tailings in flotation practices. Its flotation behavior is very important for determining the quality of concentrates of many different types of ores containing gold, copper, lead, and zinc and coal [3-5].

Many electrochemical studies of pyrite oxidation have been reported in the literature to understand the formation of surface oxidation species and their effects on the flotation behavior of pyrite [6-13]. It is well known that pyrite is a good electrocatalyst for oxygen reduction and dissolved oxygen plays an important role in pyrite oxidation and related processes such as acid mine drainage (AMD) and gold cyanidation [3, 14-21]. The oxidation and dissolution mechanism of pyrite has been investigated and it has been determined that both ferric ion and oxygen are the oxidant for pyrite but ferric ion dominates [22-24]. It is now recognized that aqueous oxidation of pyrite generally results in the production of sulfate as the ultimate oxidation product and the release of ferrous ions into solution; it also produce species such as elemental sulfur, polysulfide, hydrogen sulfide gas, ferric hydroxide precipitate, iron oxide, iron (III) oxyhydroxide and intermediates such as thiosulfate, sulfite and polythionates [25-30]

Calderia et al. [10] studied pyrite oxidation in alkaline solutions with XRD, SEM and FTIR and found that hematite is the main oxidation product on pyrite surface in hydroxide medium whereas only calcium carbonate was detected on the surface of oxidized pyrite in calcium hydroxide medium open to the atmosphere. They also observed that initial pyrite oxidation resulted in a thin oxide layer that fractured as oxidation proceeded. He et al. [2] studied effects of electrochemical potential and zinc sulphate on the floatability of pyrite at pH 9.0 and reported that zinc sulphate depressed pyrite flotation at a potential of 0.275 V (SHE) but had no or little effects at lower potentials. They speculated that this was a result of less hydroxide groups formed on pyrite surface for zinc hydroxide attachment at lower potentials. Peng et al. [31] investigated the activation of pyrite by copper ions during grinding at different potentials manipulated with H_2O_2 and dithionite with XPS and concluded that the activation is electrochemical in nature and involves the formation of Cu^+ -sulfide species. Scanning photoelectron microscopy (SPEM) and photoemission electron microscopy (PEEM) have been used to study pyrite oxidation in aqueous solutions at a submicron scale with a focus on spatially resolved surface characterization of fresh and reacted pyrite surfaces to identify site specific chemical processes [32]. The results suggest that pyrite oxidation species are heterogeneously distributed on the surface and oxidation reactions are highly site specific. Sit et al. [29] carried out spin-polarized density-functional theory (DFT) calculations of the adsorption and reactions of oxygen and water with the (100) surface of pyrite and found oxidation of the pyrite surface occurs through successive reactions of the surface with adsorbed O_2 and water molecules. Their study also revealed that the oxygens in the end oxidation product SO_4^{2-} are derived from water, not gaseous oxygen, suggesting the adsorption of water molecules plays a very important role in the process of pyrite oxidation. Jin et al. [33] used molecular dynamics simulation (MDS) and DFT quantum chemical calculations to investigate the effect of pyrite surface oxidation on interfacial water structure. They concluded that the presence of iron hydroxide is the origin of the surface hydrophilicity of the oxidized pyrite surface whereas the fresh unoxidized pyrite, polysulfide, and elemental sulfur are hydrophobic.

The influence of pyrite oxidation on flotation of other valuable sulfide minerals is an important topic for the mineral industry and has attracted many studies [34-37]. Owusu et al. [4] recently investigated the effect of pyrite on flotation of chalcopyrite and reported pyrite can be activated by copper ions released from chalcopyrite and increased surface oxidation of chalcopyrite as a result of galvanic interactions is responsible for reduced recovery of chalcopyrite.

In spite of abundant previous work, there are still unanswered questions or inconsistent information on pyrite oxidation and subsequent effects on its surface hydrophobicity and flotation behavior [6-7, 10, 27, 32-33, 35, 38-40]. This may be caused by two major reasons: 1) pyrite oxidation is complex in its nature and involves many reaction steps and products, as illustrated by Dos Santos et al. [21], Rimstidt and Vaughan [27], and Sit et al. [29]; 2) previous studies were mostly carried out with polished electrodes [6-7, 9, 12, 24]. Mechanical polishing process causes oxidation that alters electrode surface compositions, making the surface differ from the underlying substrate [41].

To study the surface oxidation of virgin pyrite surface rather than altered or contaminated surface, freshly-fractured electrode made of pyrite under controlled electrochemical potential were used in the present study. Chronoamperometry was conducted on the electrode immediately after fracture followed by cyclic voltammetry to identify surface oxidation and reduction processes and reaction products. Collectorless flotation tests of pyrite were carried out using an electrochemical microflotation cell where the potential of pyrite particle was controlled with a potentiostat.

2. EXPERIMENTAL

The freshly fractured electrodes were made of a high purity pyrite sample from Yunnan Province, China. They had the dimensions of approximately $3 \times 2 \times 10$ mm and were connected to a copper lead-wire through the use of conducting silver epoxy. The electrode was then mounted at the end of a 7 mm diameter glass tube with non-conducting epoxy (Torr Seal, Varian Vacuum Products). After the electrode was inserted into the electrochemical cell, the projecting portion was subjected to a sharp blow through a glass rod resting on it to create a freshly-fractured surface which was usually flush with the epoxy. The ring-disc electrodes were constructed using a similar procedure described by Ahlberg and Boo [42]. Solutions in the electrochemical cell were made of 0.05 M sodium tetraborate with a buffered pH 9.2 and 0.05 M acetate and 0.05 M acetic acid with a buffered pH 4.6 and purged with N_2 for at least 1 h prior to each experiment.

A Pine RDE-4 double potentiostat was used to conduct chronoamperometry and cyclic voltammetry studies with freshly fractured electrodes. The voltammograms of pyrite disc electrode were conducted at a potential sweep rate of 20 mV/s and currents on the gold ring electrode were recorded on the second-cycle, unless otherwise specified. A saturated calomel electrode (SCE) was used as the reference electrode and a platinum wire as the counter electrode. Potentials are reported on the standard hydrogen electrode (SHE) scale by adding 0.245 V. X-ray photoelectron spectroscopy (XPS) measurements were performed in a commercial PHI 5400 spectrometer under a pressure in the 10^{-7} Pa range. The photoelectron spectra were recorded with monochromatized Al K α radiation (1486.6 eV). The ratio of oxygen and oxidized sulfur was determined based on the binding energy intensity at 531.5 eV in the O 1s spectra and that at 168.5 eV in the S 2p $_{1/2}$ spectra. Microflotation tests were performed with the 65-150 mesh pyrite sample for three minutes in an electrochemical microflotation cell [41] using a potentiostat for control of solution potential. All experiments were carried out in the buffer solutions described above at room temperature of approximately 20° C.

3. RESULTS AND DISCUSSION

Chronoamperometry is an electrochemical technique in which an electrical current resulting from faradaic processes is measured as a function of time. Figure 1 shows the chronoamperometry curves of pyrite electrodes held at different electrochemical potentials during and after in-situ fracture at pH 9.2. The formation of fresh pyrite surface upon fracture creates a step-wise change in the potential of working electrode of pyrite. The subsequent faradaic process due to electron transfer at the pyrite-solution interface causes a current decaying exponentially as a function of time as described in the Cottrell equation. Since the pyrite electrode was held at a given potential prior to fracture the Faradaic process on pyrite observed after fracture arises from the difference between the applied potential and the potential the freshly created pyrite surface assumes at the instant of fracture. Thus an anodic current represents an oxidation reaction and a cathodic current indicates a reduction process. A zero current suggests pyrite does not undergo electrochemical reaction and is thermodynamically stable at that particular potential. As can be seen in Figure 1, as the potential increases from -0.55 V to 0.45 V, the current changes in its magnitude as well as its sign. At potentials more negative than -0.28 V, cathodic reduction takes place on pyrite and the reaction kinetics increases with the magnitude of the negative potential. At the potentials less negative than -0.28 V or at positive potentials, pyrite undergoes oxidation reactions and oxidation is faster at less negative or more positive potentials.

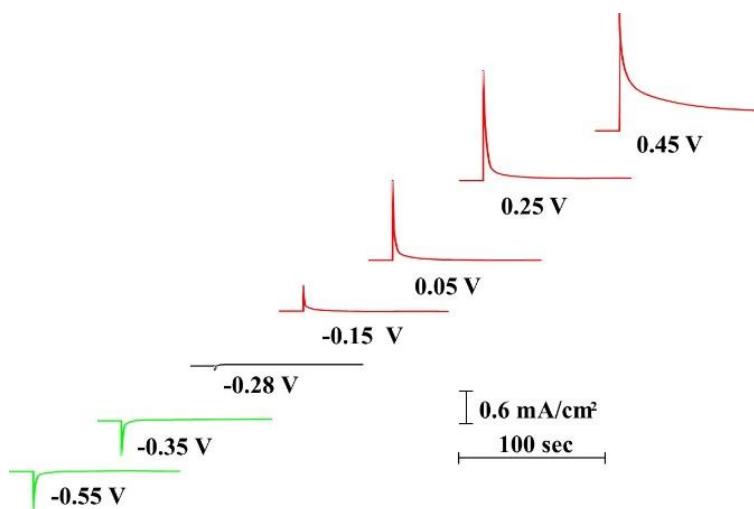


Figure 1. Chronoamperometry curves of pyrite fractured at different potentials at pH 9.2.

It is important to note that Figure 1 indicates that freshly fractured pyrite surface at -0.28 V at pH 9.2 showed nearly zero current. In other words, fresh pyrite surface is stable at -0.28 V at pH 9.2. A similar stable potential was identified to be at 0 V at pH 4.6. Figure 2 shows the Eh-pH diagram for the pyrite-H₂O system [43]. It is obvious that the stable potentials are right in the middle of the thermodynamic stability domain of pyrite, indicating 1) the chronoamperometry results are consistent with thermodynamics of the pyrite and water system; 2) fresh pyrite surface readily oxidizes in aqueous solutions open to air. This is of particular relevance to grinding operations since it suggests even the pyrite in freshly ground slurry is oxidized due to higher pulp potentials than the stable

potential [4, 44-45] and therefore have impacts on its natural floatability and interactions with flotation reagents. The chronoamperometry data is in contrast with the established mixed potential values of pyrite, which are 0.2 V at pH 9.2 and 0.6 V at pH 4.6 [46-47], confirming pyrite readily oxidizes in aqueous solutions under normal ambient conditions.

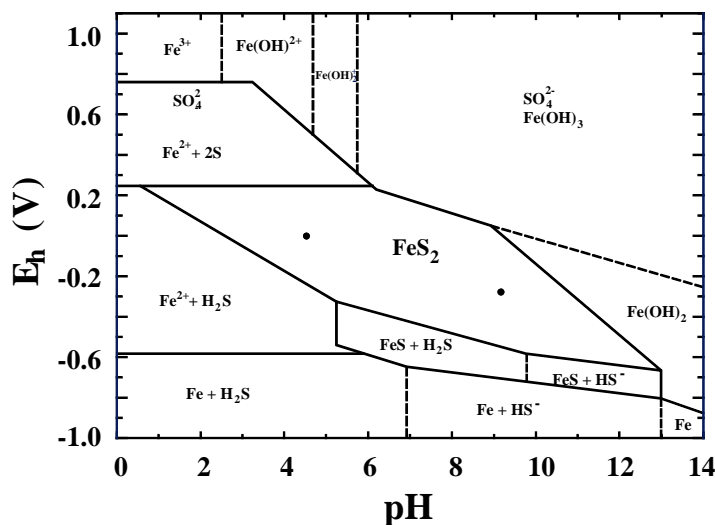
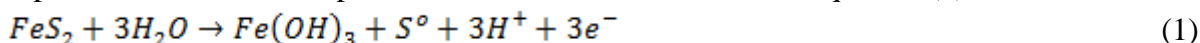
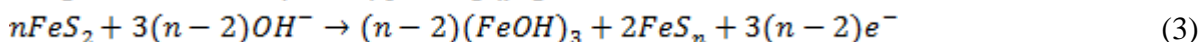
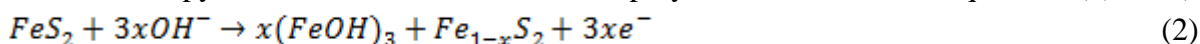


Figure 2. Eh-pH diagram for the FeS₂-H₂O system and for 10⁻⁵ M dissolved species [43]. Solid circles represent the stable potentials identified in this study.

Cyclic voltammetry has been widely used to investigate electrochemical reactions of pyrite and other sulfide minerals [6-8, 48-54] but results differ considerably, particularly on which anodic peak represents the oxidation of pyrite itself. For example, Hamilton and Woods [6] reported that pyrite oxidation takes place at potentials above 0.2 V whereas oxidation of ferrous to ferric ion occurs at approximately -0.05 V at pH 9.2. On the other hand, Ahlberg et al. [7] conducted cyclic voltammetry on pyrite in alkaline solutions and concluded the oxidation of pyrite starts at about 0 V (SCE) or 0.25 V (SHE) at pH 11, suggesting pyrite oxidation occurs only at potentials above approximately 0.40 V (SHE) at pH 9.2 under the assumption that oxidation reaction follows equation (1) [7, 54, 56-57].



In fact, Velasquez et al. [50] observed an oxidation peak at 0.4 V at pH 9.2 and they attributed it to the oxidation of pyrite to metal-deficient sulfide or polysulfide as shown in Equations (2) and (3).



But their XPS results indicate no polysulfides were detected after oxidation and they claim metal-deficient sulfide is a more likely product. The inconsistency on pyrite oxidation potential in literature may be related to the fact that most of voltammetry studies on pyrite were performed with polished electrodes on which oxidation reactions have already occurred during polishing and electrode surface have been covered by oxidation products such as ferric hydroxide prior to voltammetry experiments [58-59]. With freshly fractured electrode used in the present study this problem is eliminated when the electrode is held at the stable potential during fracture. Figure 3 shows the voltammetry curves obtained with pyrite electrode at pH 9.2 after fresh fracture at -0.28V. To study

the oxidation of fresh pyrite surface, the potential sweep initiated anodically from -0.28 V and the potential sweep was limited to the range of -0.55 V and +0.55 V to avoid excessive reduction or oxidation reactions of pyrite. As can be seen in Figure 3, a significant oxidation current was observed at approximately -0.2 V on the first voltammogram and formed an anodic peak at 0 V. Since fresh pyrite surface is free of any other species, this oxidation must arise from the oxidation of pyrite itself. During the second and third potential sweep, an anodic peak at -0.1 V appeared, which has been identified to be the oxidation of ferrous to ferric ion by a number of electrochemical and XPS studies [6-7, 10, 53]. An important finding from Figure 3 is that the positions of anodic peaks representing ferrous ion oxidation and pyrite oxidation are very close to each other. Another noteworthy feature of second and third voltammogram in Figure 3 is that the anodic oxidation peak at 0 V disappeared, suggesting pyrite may be passivated by the presence of iron hydroxide [58-59]. It is thus not surprising that previous investigator using polished electrodes did not observe pyrite surface oxidation at a low potential near 0 V until at much higher potentials where aggressive oxidation takes place as described in Equation (4) [6-7, 56-57, 59].

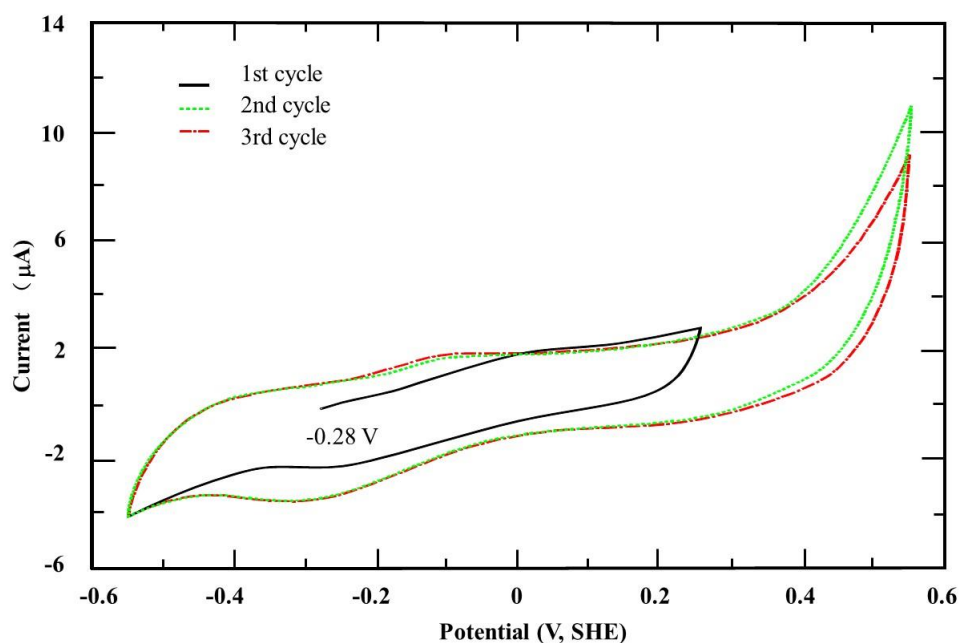
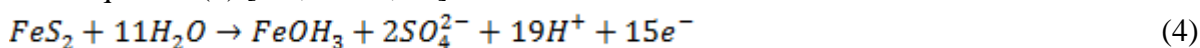


Figure 3. Voltammograms of pyrite freshly fractured at -0.28 V at pH 9.2

Figure 4 shows the first two consecutive voltammetry curves after fresh fracture at -0.45 V. The chronoamperometry curve obtained after fracture at -0.45 V is also shown in Figure 4 as the inset. Based on the chronoamperometry curve one can determine the charge density associated with the cathodic reduction process to be 106 mC/cm² for the first 2 minutes after fracture, which corresponds to a reaction involving less than a monolayer of pyrite [41]. The voltammetry curve started at -0.45 V to oxidize reduced species formed after fracture and an initial anodic current was observed at -0.25 V and formed a peak at about 0 V. Integrating the current from -0.25 V to 0.25 V gave rise to a charge density of 241 mC/cm² for the anodic oxidation during the positive going potential sweep, which is

substantially greater than the charge density of 106 mC/cm^2 observed on the chronoamperometry curve. This difference can only be attributed to the oxidation of pyrite itself, confirming that pyrite oxidizes in a low potential region represented by the anodic peak at 0 V.

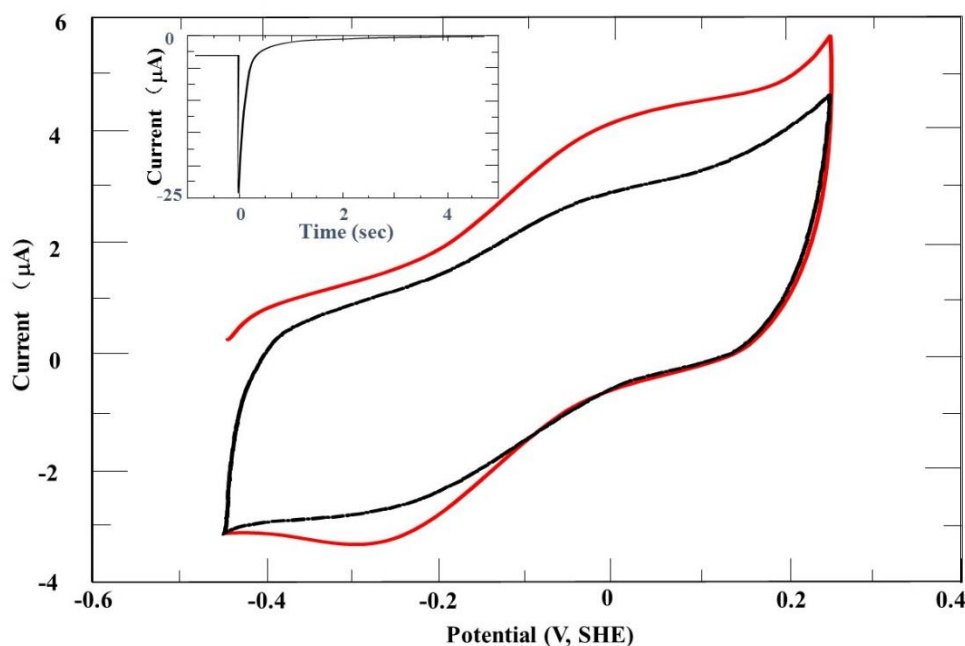


Figure 4. Voltammograms of pyrite freshly fractured at -0.45 V at pH 9.2

The results shown in Figures 1, 3, and 4 strongly indicate that fresh pyrite undergoes surface oxidation at a much lower potential than previously reported [6-7, 56-57], which is however in good agreement with a recent study by Mu et al. [54] using fractured electrodes. This finding is important because the natural floatability or collectorless flotation behavior of pyrite is important for industrial flotation practices where sulfide minerals of copper, lead, zinc, nickel, etc. are selectively floated away from pyrite to generate high quality concentrates of valuable sulfide minerals [6-7, 60-63]. A good understanding of pyrite oxidation potential at which hydrophobic species forms is a prerequisite to controlling its natural hydrophobicity to minimize its flotation recovery.

To investigate the collectorless flotation behavior of pyrite a series of microflotation tests were conducted with 100-200 mesh pyrite particles at different pH's. Figure 5 shows the flotation recovery of pyrite as a function of solution potential at pH 4.6, 6.8, 8.0, and 9.2 in the absence of sulfide collectors such as xanthate. A significant flotation recovery of pyrite was observed over a range of potential that is dependent on solution pH. In general the potential range for flotation is wider and the maximum flotation recovery is greater at lower pH's. The collectorless flotation recovery of pyrite is 80-90% in the potential range of 0 - 0.4 V at pH 6.8 and approximately 90-95% over -0.05 – 0.45 V at pH 4.6. This is because a larger amount of hydrophilic species such as ferrous and ferric hydroxides precipitates on pyrite surface and reduces its hydrophobicity at higher pH's as indicated in Equations 1-4 [64-67]. The lower flotation limit is determined by the potential at which one or more of reactions described by Equations 1-3 takes place. For example, pyrite starts to show floatability at approximately -0.1 V at pH 9.2, which is consistent with the chronoamperometry and voltammetry results discussed

above. The upper flotation limit is controlled by aggressive pyrite oxidation represented by Equation (4) that generates soluble sulfate rather than hydrophobic sulfur species and hydrophilic iron hydroxides [68-70].

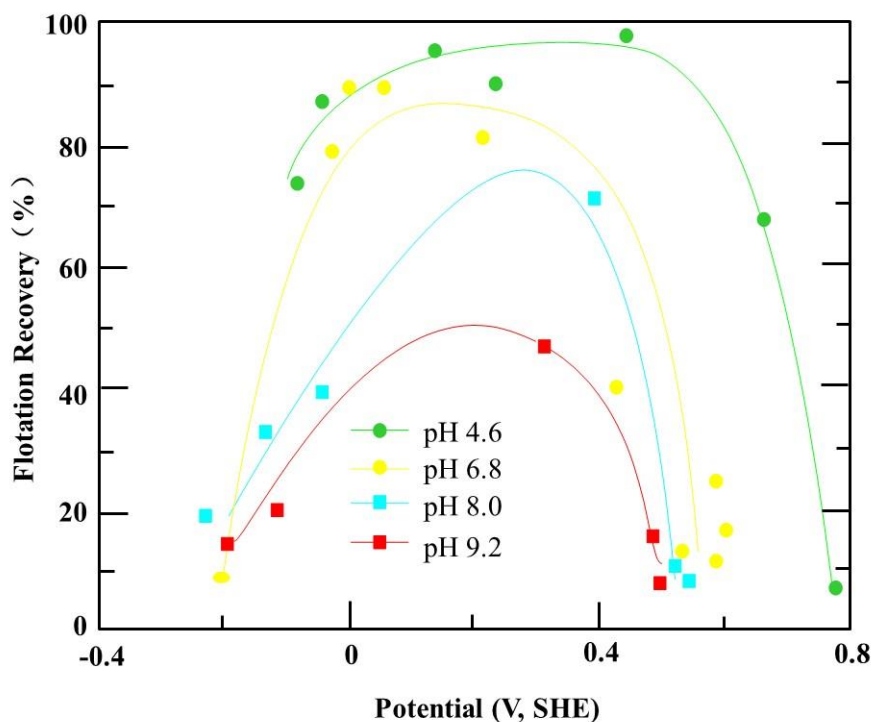


Figure 5. Pyrite flotation recovery as a function of solution potential at different pH's

Figure 5 indicates that pyrite flotation recovery is strongly dependent on solution pH and Eh, suggesting that the surface hydrophobicity of pyrite is a function of relative abundance of hydrophobic sulfur containing species such as metal deficient sulfide, polysulfide, or elemental sulfur and hydrophilic species such as ferric hydroxide $\text{Fe}(\text{OH})_3$. To provide more evidences for this relationship, microflotation tests with pyrite were carried out in the presence of $5 \times 10^{-4} \text{ M}$ EDTA and 30 ppm kerosene, respectively and the results are shown in Figure 6. EDTA is an iron chelating agent that can remove iron species from pyrite surface whereas kerosene was used as flotation collector or surface hydrophobizing agent to enhance pyrite surface hydrophobicity [31, 45]. Figure 6 shows that use of EDTA significantly increased the flotation recovery of pyrite at a given potential but it did not change the onset potential of pyrite flotation at pH 9.2, which is consistent with the previous conclusion that the source of pyrite hydrophobicity is the hydrophobic sulfur species and the formation of iron hydroxides from pyrite oxidation reduces pyrite surface hydrophobicity. By removing iron hydroxides on pyrite surface using EDTA to expose the underlying hydrophobic sulfur species, pyrite surface hydrophobicity can be enhanced. The fact that the onset potential of flotation did not change confirms that pyrite is not naturally hydrophobic and its hydrophobicity indeed arises from its oxidation process that produces a sulfur rich surface. Similar behavior has also been observed by He et al. [2], Peng et al. [31], Mu et al. [59], Lopez Valdivieso et al. [66], and He et al. [71] in their studies of pyrite

flotation with xanthate and its depression with different reagents. It should be noted, however, that although Figure 5 shows higher pH's reduced floatability of pyrite without collector, this is not true for pyrite in sulfide flotation practices with collector. It has been observed that pyrite floatability may be increased in alkaline solutions when xanthate collectors are present to float other sulfides containing base metals such as Pb, Cu, and Zn due to the inadvertent activation of pyrite by Cu^{2+} or Pb^{2+} at higher pH's [4, 72-73].

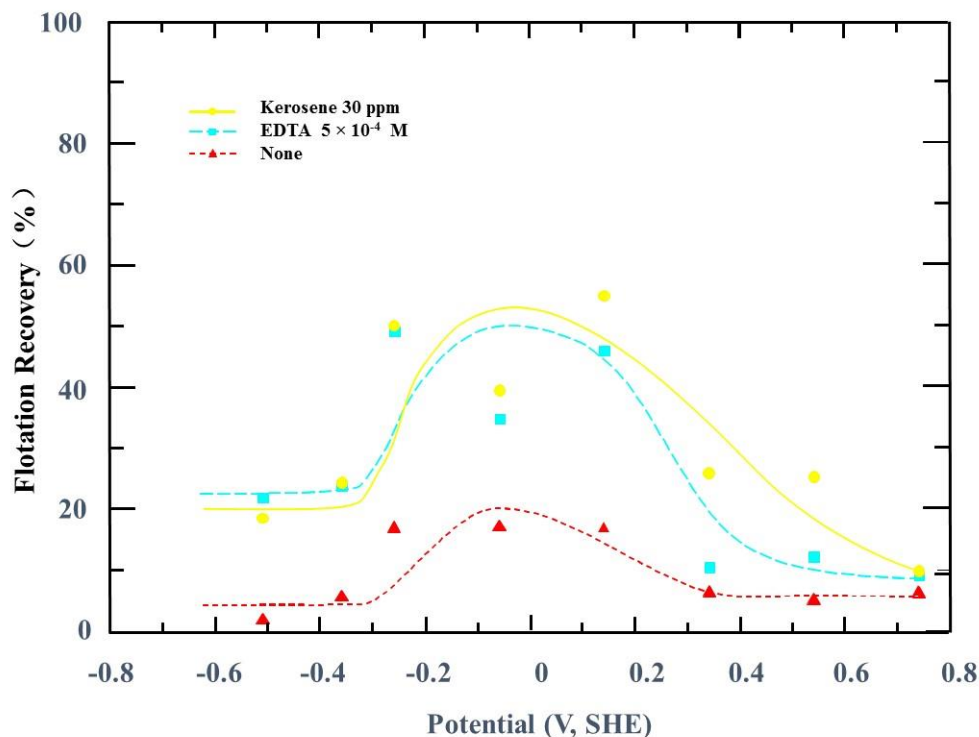


Figure 6. Pyrite flotation recovery as a function of solution potential at pH 9.2 in the presence of 5×10^{-4} M EDTA and 30 ppm kerosene

While it has been claimed that flotation or depression of pyrite depends upon the balance of hydrophobic and hydrophilic species on the surface and several ionic equilibria can modify pyrite surfaces by a change in pH [59, 66,71], no specific relationship between pyrite floatability and the relative abundance of hydrophobic and hydrophilic species has been established. Figure 7 shows the flotation recovery of pyrite as a function of the ratio of oxygen and oxidized sulfur based on XPS analysis results obtained at different solution pH's and oxidation potentials. There appears to be a negative linear relationship between flotation recovery and the oxygen/oxidized sulfur ratio. Less oxygen or more oxidized sulfur on pyrite surface results in greater hydrophobicity and thus higher flotation recovery. This finding is consistent with the other results shown above and in previous studies since oxygen concentration is an indication of the amount of hydroxides whereas oxidized sulfur represents the amount of hydrophobic sulfur-rich species on pyrite after oxidation [10, 50, 69-70]. A higher oxygen/oxidized sulfur ratio implies a greater amount of hydroxides and/or a lower concentration of hydrophobic sulfur oxidation species which lead to weaker surface hydrophobicity. The effect of oxygen on pyrite flotation by collectors has been studied by other investigators and their

results are in agreement with the present study. For example, Shen et al. [74] and Owusu et al. [75] reported the formation of hydrophilic species such as copper/iron hydroxide and sulfate may prevent or reduce the adsorption of collector on pyrite. In fact, it has been observed that improved separation of pyrite from sphalerite, galena and gold may be achieved under oxidizing conditions by reducing pyrite floatability [37, 76]

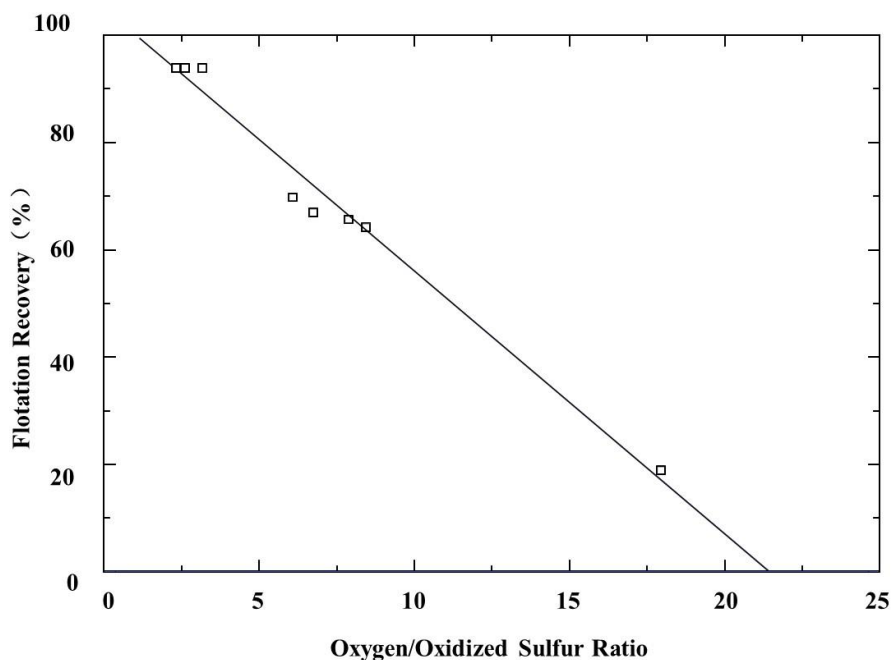


Figure 7. Flotation recovery of pyrite as a function of oxygen/oxidized sulfur ratio.

4. CONCLUSIONS

Based on above experimental results and discussion, the following conclusions can be drawn:

1. Freshly fractured pyrite surface is considerably different from polished surface and the latter is not suitable for studying oxidation of true pyrite surface.
2. Surface oxidation of pyrite that is responsible for inducing surface hydrophobicity or collectorless flotation behavior occurs at a potential close to the equilibrium potential of ferrous and ferric redox couple and is often masked by the oxidation of ferrous to ferric ion.
3. Fresh pyrite oxidizes and consequently induces surface hydrophobicity at potentials substantially lower than the thermodynamic potential for the formation of elemental sulfur, suggesting that metal deficient sulfides or polysulfides are likely oxidation species responsible for collectorless flotation behavior of pyrite.
4. The electrochemically stable potential of pyrite identified by chronoamperometry and voltammetry studies is consistent with the thermodynamic data of $\text{FeS}_2 - \text{H}_2\text{O}$ system.
5. Microflotation test results have shown considerable collectorless flotation recovery of pyrite, especially at neutral and acidic pH's and a definite correlation between flotation recovery of pyrite and relative abundance of oxygen and oxidized sulfur species has been established.

6. This study clearly indicates the importance of controlling solution pH and Eh to achieve the best possible separation of valuable metal sulfides from pyrite or pyrite rejection from coal in industrial flotation practices.

References

1. M. Dimitrijevic, M.M. Antonijevic, Z. Jankovic, *Hydrometallurgy*, 42 (1996) 377.
2. S. He, W. Skinner, D. Fornasiero, *Int. J. Miner. Process.*, 80 (2006) 169.
3. H.Tan, D.Feng, J.S.J. Deventer, G.C.Lukey, *Int. J. Miner. Process.*, 80 (2006) 153.
4. C.Owusu, S.B.Abreu, W. Skinner, J. Addai-Mensah, M. Zanin, *Miner. Eng.*, 55 (2014) 87.
5. Rabies, A., Albijanic, B., Eksteen, J.J. *Miner. Eng.*, 112 (2017) 68.
6. I.C. Hamilton, R. Woods, *J. Electroanal. Chem.*, 118 (1981) 327.
7. E. Ahlberg, K.S.E. Forssberg, X. Wang, *J. Appl. Electrochem.*, 20 (1990) 1033.
8. F.M. Doyle, A.H. Mirza, In: Woods, R., Doyle, F.M., Richardson, P. (Eds.), *Proc. 4th International Symposium on Electrochemistry in Mineral and Metal Processing*. The Electrochem. Soc., pp. 203–214, 1996.
9. G.H. Kelsall, Q. Yin, D.J. Vaughan, England, K.E.R. In: Woods, R., Doyle, F.M., Richardson, P. (Eds.), *Proc. 4th International Symposium on Electrochemistry in Mineral and Metal Processing*. The Electrochemical Society, pp. 131–142, 1996.
10. C.L. Caldeira, V.S.T. Ciminelli, A. Dias, K. Osseo-Asare, Pyrite oxidation in alkaline solutions: nature of the product layer, *Int. J. Miner. Process.*, 72 (2003) 373.
11. F.D. Ardejani, B.J. Shokri, M. Bagheri, E. Soleimani, *Environ. Earth Sci.*, 61 (2010) 1547.
12. H. Sun, M. Chen, L. Zou, R. Shu., R. Ruan, *Hydrometallurgy*, 155 (2015) 13.
13. H.-Y. Sun, Q-Y. Tan, Y. Jia, R-B. Shu, S.-P. Zhong, R.-M. Ruan, *Rare Metals*, 8 (2017) 1.
14. T. Biegler, *J. Electroanal. Chem.*, 70 (1976) 265.
15. K.C.Pillai, J.O. M.Bockris, *J. Electrochem. Soc.*, 131 (1984) 568.
16. C.O. Moses, N.D. Kirk, J.S. Herman, A.L. Mills, *Geochim Cosmochim Acta.*, 51(6) (1987) 1561.
17. G.A. Kudaikulova, M.R. Tarasevich, K.A. Radyushkina, *Elektrokhimiya*, 26 (1990) 1025.
18. G.Q. Liu, W.T. Yen, *Miner. Eng.*, 8 (1-2) (1995) 111.
19. H. Tan, D. Feng, G.C. Lukey, J.S.J. van Deventer, *Hydrometallurgy*, 78 (3-4) (2005) 226.
20. J. Satur, J. Hiroyoshi, M. Tsunekawa, M.Ito, H. Okamoto, *Int. J. Miner. Process.*, 83 (2007) 116.
21. E. C. Dos Santos, J. C. De Mendonça Silva, H.A. Duarte, *J. Phys. Chem. C*, 120 (2016) 2760.
22. M.A. McKibben, H.L. Barnes, *Geochim Cosmochim Acta.*, 50 (1986) 1509.
23. R.V. Nicholson, R.W. Gillham, E.J.Reardon, *Geochim Cosmochim Acta.*, 52 (1988) 1077.
24. P.R. Holmes, F.K. Crundwell, *Geochim Cosmochim Acta.*, 64 (2000) 263.
25. A. N. Buckley, R. Woods, *Appl. Surf. Sci.*, 27 (1987) 437.
26. V. P. Evangelou, *Pyrite Oxidation and Its Control*. CRC Press, NewYork, 1995.
27. J. D.Rimstidt, D. J. Vaughan, *Geochim. Cosmochim. Acta*, 67 (2003) 873–880.
28. O. Bicak, Z. Ekmekci, *Miner. Eng.*, 36-38 (2012) 279.
29. P. H.-L. Sit, M.H. Cohen, A. Selloni, *J. Phys. Chem. Letters*, 3 (2012) 2409.
30. K. Park, J. Choi, A. Gomez-Flores, H. Kim, *Mater. Trans.*, 56 (2015) 435.
31. Y. Peng, B. Wang, A. Gerson, *Int. J. Miner. Process.*, 102-103 (2012) 141.
32. A.P. Chandra, A.R. Gerson, *Surf. Sci. Rep.*, 65 (2010) 293.
33. J. Jin, J.D. Miller, L.X. Dang, C.D. Wick, *Int. J. Miner. Process.*, 139 (2015) 64.
34. M. Xu, J.A. Finch, S.R. Rao, D. Lin, *Miner. Eng.*, 8 (1995) 1159.
35. N.P. Finkelstein, *Int. J. Miner. Process.*, 52 (1997) 81.
36. Y. Peng, S. Grano, D. Fornasiero, J. Ralston, *Int. J. Miner. Process.*, 69 (2003a) 87.
37. Y. Peng, S. Grano, D. Fornasiero, J. Ralston, *Int. J. Miner. Process.*, 70 (2003b) 67.

38. A.N. Buckley, R. Woods, In: Richardson, P.E., Srinivasan, S., Woods R. (Eds.), *Electrochemistry in Mineral and Metal Processing*. The Electrochemical Society, Pennington, NJ, pp. 286-302. 1984.
39. J. Pang, A. Briceno, S. Chander, *J. of Electrochem. Soc.*, 137 (1990) 3447.
40. S. Chander, A. Briceno, and J. Pang, *Miner. and Metallur. Process.*, 10 (1993) 113-118.
41. P.E. Richardson, R.-H. Yoon, In: Hiskey, J.B., Warren, G.W. (Eds.), *Hydrometallurgy, Fundamentals, Technology and Innovations*, Society for Mining, Metallurgy, and Exploration, Littleton, CO., pp. 101-118, 1993.
42. E. Ahlberg, A.E. Broo, *Int. J. Miner. Process.*, 46 (1996) 73.
43. D. Kocabag, H.L. Shergold, G.H. Kelsall, *Int. J. Miner. Process.*, 29 (1990) 211.
44. S. Grano, *Miner. Eng.*, 22 (2009) 386.
45. Y. Peng, S. Grano, *Miner. Eng.*, 23 (2010) 600.
46. S. Chander, A. Briceno, *Miner. Metall. Process.*, 4 (1987) 171.
47. S.R. Rao, J.A. Finch, *Can. Metall. Q.*, 27 (1988) 253.
48. N.D. Janetski, S.I. Woodburn, R. Woods, *Int. J. Miner. Process.*, 4 (1977) 227.
49. E. Ahlberg, A.E. Broo, *J. Electrochem. Soc.*, 144 (1997) 281.
50. P. Velasquez, D. Leinen, J. Pascual, J.R. Ramos-Barrado, P. Grez, H. Gomez, R. Schrebler, R. Del Rio, R. Cordova, *J. Phys. Chem. B*, 109 (2005) 4977.
51. D. Wang, L. Fan, C. Fan, *Adv. Mater. Res.*, 554-556 (2012) 379.
52. M. Eghbalnia, D.G. Dixon, *J. Solid State Electrochem.*, 17 (2013) 235.
53. Y. Mu, Y. Peng, R.A. Lauten, *Electrochimica Acta*, 174 (2015) 133.
54. Y. Mu, L. Li, Y. Peng, *Miner. Eng.*, 101 (2017) 10.
55. L. Li, I. Bergeron, A. Ghahreman, *Electrochimica Acta*, 245 (2017) 814,
56. B.F. Giannetti, S.H. Bonilla, C.F. Zinola, T. Raboczky, *Hydrometallurgy* 60 (2001) 41.
57. G.-H. Gu, X.-J. Sun, K.-T. Hu, J.-H. Li, G.-Z. Qiu, *Trans. Nonferrous Metals Soc. China*, 22 (2012) 1250.
58. G.-X. You, C.-C. Yu, Y. Lu, Z. Dang, *Electrochim. Acta*, 93 (2013) 65.
59. Y. Mu, Y. Peng, R.A. Lauten, *Miner. Eng.*, 96-97 (2016) 143.
60. R. Woods, *Int. J. Miner. Process.*, 72 (2003) 151.
61. H. Moslemi, P. Shamsi, F. Habashi, *Miner. Eng.*, 24 (2011) 1038.
62. W. Qin, X. Wang, L. Ma, F. Jiao, R. Liu, C. Yang, K. Gao, *Miner. Eng.*, 74 (2015) 99.
63. W. Chimonyo, J. Wiese, K. Corin, and C. O'Connor, *Miner. Eng.*, 109 (2017) 135.
64. J.O. Leppinen, *Int. J. Miner. Process.* 30 (1990) 245.
65. X.H. Wang, K.S.E. Forssberg, *Int. J. Miner. Process.*, 33 (1991) 275.
66. A. Lopez Valdivieso, A.A. Sanchez Lopez, S. Song, *Int. J. Miner. Process.*, 77 (2005) 154.
67. M.C. Fuerstenau, G.J. Jameson, R.H. Yoon, *Froth Flotation: A Century of Innovation*. Society for Mining, Metallurgy, and Exploration, Littleton, Colo., 2007.
68. C.J. Martin, R.E. McIvor, J.A. Finch, S.R. Rao, *Miner. Eng.*, 4 (1991) 121.
69. G.D. Senior, W.J. Trahar, *Int. J. Miner. Process.*, 33 (1991) 321.
70. R.S.C. Smart, *Miner. Eng.*, 4 (1991) 891.
71. S. He, D. Fornasiero, W. Skinner, *Miner. Eng.*, 18 (2005) 1208.
72. T.K. Dichmann, J.A. Finch, *Miner. Eng.*, 14 (2001) 217.
73. G.J. Barker, A.R. Gerson, J.F. Menuge, *Int. J. Miner. Process.*, 128 (2014) 16.
74. W.Z. Shen, D.Fornasiero, J. Ralston, *Miner. Eng.*, 11 (1998) 145.
75. C. Owusu, J. Addai-Mensah, D. Fornasiero, M. Zanin, *Adv. Powder Technol.*, 24 (2013) 801.
76. A. Boulton, D. Fornasiero, J. Ralston, *Miner. Eng.*, 14 (2001) 1067.